

Frequency Splitting Analysis of Wireless Power Transfer System Based on T-type Transformer Model

Lan Jianyu¹, Tang Houjun¹, Gen Xin¹

¹*Department of Electrical Engineering, Shanghai Jiao Tong University,
Dongchuan Rd. No. 800, 200240 Shanghai, China
jianyu_lan@163.com*

Abstract—Frequency splitting is a key characteristic of wireless power transfer system. With the increases of coupling coefficient, the power transferred to load drops sharply. The resonant frequency splits from one into two within splitting region. Previous reports about frequency splitting mainly focused on the analysis of coupled mode theory or the solutions of ridge equations. In this work, we presented the analytical results based on a simply T-type circuit model. With impedance analysis, the even and odd splitting frequencies were derived. In addition, the frequency splitting phenomena were analysed with output voltage curves at different coupling by the aid of simulation. Furthermore, the frequency splitting and the frequency bifurcation discussed frequently in inductively coupled wireless power transfer system were analysed comparatively based on the circuit model. Then, a half-bridge inverter based wireless power system was constructed to demonstrate the experimental results. Finally, the simulation and experimental results validated the theoretical analysis.

Index Terms—Frequency splitting, wireless power transfer, resonant frequency

I. INTRODUCTION

In recent years, the wireless power transfer (WPT) technologies have been the growing hot topics for researchers. WPT applications can be found in a wide range from implanted biomedical devices, consumer electronics' chargers and vehicle battery charges [1]–[3]. Among WPT technologies, the magnetic resonance coupling method has a better promise because of its long transfer distance and high efficiency [1], [4]. MIT groups experimentally demonstrated this power transfer method over distances up to 8 times the radius of the coils. A 60 watts bulb was lighted over distances of more than two meters [5], [6].

For magnetic resonance coupling WPT systems, when moving the two coils to be close step by step and when they are close enough, the power transferred to load drop sharply. This is because the resonant frequency has been changed when the coupling of coils becomes stronger. This phenomenon is called frequency splitting which is defined and explained in [7], [8]. When the coupling between the

transmitter coil and receiver coil increases and is greater than a critical frequency, the resonance frequency will split into two resonant frequencies, the odd frequency and the even frequency; thus, the load voltage will change from a single-peak curve to a double-peak curve. Frequency splitting is an important issue, related to the power transfer efficiency and capability of WPT systems. Works about frequencies splitting were reported widely based on coupled mode theory (CMT) and circuit theory [9]–[15]. In [7], the directional coupler-based method was suggested to track the splitting frequency in a magnetic resonance system. Reference [16] applied a root locus method to explain the double voltage-peak of frequency splitting of WPT systems. In [17], an asymptotic coupled mode theory method has been used to analyse the frequency splitting phenomena in contactless power transfer systems. The critical coupling coefficient has been derived based on the energy equations. In [18], an exact analysis about frequency splitting of the symmetrical and unsymmetrical contactless power transfer systems is shown in detail. However, related reports based on CMT [5], [6], [17] presented by physicists cannot be understood well by researchers of electrical engineering. On the other hand, lots of research just shows the phenomena of frequency splitting with double-peak characteristic of output power curve [9]–[14]; the studies seldom give detailed analysis on how the splitting frequency changes, what the even and odd frequencies are and what the relationship of the splitting frequency to main circuit parameters is.

In this work, first, a simple T-type transformer model is introduced to analyse the magnetic coupling WPT system. Then, the odd frequency and even frequency are determined using simple equations by the impedance analysis of T-type transformer model. Then, an analysis about frequency splitting based on simulation is also presented. At last, a WPT prototype is constructed. The driver of a WPT system is important concerning the efficiency of a WPT system. Here, we used the half-bridge inverter to drive the source coil. The zero voltage switching condition is discussed as well. Then, the experimental results validate the theoretical analysis. This paper is organized as following. In Section II the methods are presented. In Section III, the analysis based on the experimental results is given. Finally, the discussion and conclusions are given in the Section IV.

Manuscript received April 10, 2013; accepted September 25, 2013.

This work is supported by the National Natural Science Fund of China (51277120) and ITER Special Project (2011GB113005). This work is also supported by State Energy Smart Grid R&D Center (China, Shanghai).

II. METHODS

A. CMT Mode

The typical WPT system is shown in Fig. 1, where L_1 and L_2 represent the source coil and device coil, respectively; R_1 and R_2 are their internal resistances, respectively; the capacitors C_1 and C_2 are connected in series both in source coil and device coil to form a series-tuned resonant converter. M is the mutual inductance between coils, R_L is the load resistance, and U_{in} is the source voltage.

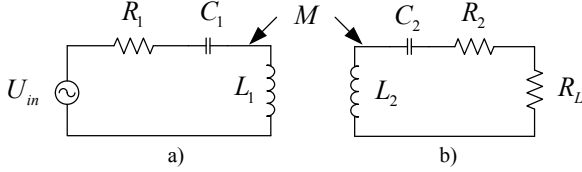


Fig. 1. Topology of WPT system.

The WPT system is described by using CMT theory [2], [3]

$$\frac{d}{dt} \begin{bmatrix} a_1(t) \\ a_2(t) \end{bmatrix} = \begin{bmatrix} j\omega_0 - \Gamma_1 & jK \\ jK & j\omega_0 - (\Gamma_2 + \Gamma_L) \end{bmatrix} \begin{bmatrix} a_1(t) \\ a_2(t) \end{bmatrix} + \begin{bmatrix} A s e^{j\omega t} \\ 0 \end{bmatrix}, \quad (1)$$

where $a_1(t)$ and $a_2(t)$ are the magnetic field amplitudes of the primary and secondary coils, respectively; Γ_1 and Γ_2 are the intrinsic loss coefficient of the two coils, Γ_L is the intrinsic loss coefficient about the load resistance; ω_0 is the nature resonant frequency of coils; and K is the coupling coefficient between two coils. The load power is expressed as following [4], [5]

$$P_L = \frac{2\Gamma_L K^2 A_s^2}{\left[K^2 + \Gamma_1(\Gamma_2 + \Gamma_L) - (\omega - \omega_0)^2 \right]^2 + (\Gamma_1 + \Gamma_2 + \Gamma_L)^2 (\omega - \omega_0)^2}, \quad (2)$$

The splitting equation is defined as [14]

$$\frac{\partial P_L}{\partial \omega} = 0. \quad (3)$$

Substituting (2) into (3), the odd and even splitting can be derived [14]

$$\omega = \omega_0 \pm [K^2 - 0.5\Gamma_1^2 - 0.5(\Gamma_2 + \Gamma_L)^2]^{0.5}. \quad (4)$$

B. T-type Transformer Model Method

The circuit in Fig. 1 transferred to T-type transformer model is shown in Fig. 2.

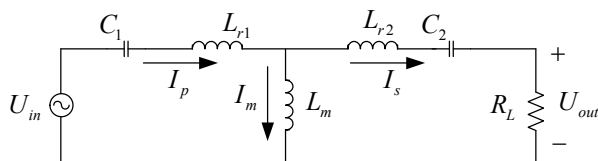


Fig. 2. T-type transformer model of WPT system.

From Fig. 2, the impedance of the transformer is expressed

as (5) and (6):

$$Z_1 = \frac{1}{sC_1} + sL_{r1} + sL_m / (sL_{r2} + \frac{1}{sC_2} + R_L), \quad (5)$$

$$Z_1 = \frac{1}{sC_1} + sL_{r1} + \frac{s^3 L_{r2} L_m C_2 + s^2 L_m C_2 R_L + sL_m}{s^2 L_{r2} C_2 + s^2 L_m C_2 + sR_L C_2 + 1}. \quad (6)$$

Then, the current of source coil is

$$I_p = \frac{U_{in}}{Z_1}. \quad (7)$$

Using Kirchhoff's current/voltage laws, the circuit equations are shown from (8) to (10):

$$I_p \left(\frac{1}{sC_1} + sL_{r1} \right) + sI_m L_m = U_{in}, \quad (8)$$

$$I_p \left(\frac{1}{sC_1} + sL_{r1} \right) + I_s \left(\frac{1}{sC_2} + sL_{r2} + R_L \right) = U_{in}, \quad (9)$$

$$I_m + I_s = I_p. \quad (10)$$

Substituting (8) and (9) into (10), the device coil current I_s and output voltage U_{out} can be derived as following:

$$I_s = I_p \frac{sL_m}{\frac{1}{sC_2} + sL_{r2} + sL_m + R_L}, \quad (11)$$

$$U_{out} = I_p \frac{sL_m R_L}{\frac{1}{sC_2} + sL_{r2} + sL_m + R_L}. \quad (12)$$

Define the voltage gain as

$$Gain = \frac{U_{out}}{U_{in}}. \quad (13)$$

Substituting (7) and (12) into (13), the voltage gain is derived

$$Gain = \frac{sL_m R_L}{\left(\frac{1}{sC_2} + sL_{r2} + sL_m + R_L \right)} \times \frac{1}{\left(\frac{1}{sC_1} + sL_{r1} + \frac{s^3 L_{r2} L_m C_2 + s^2 L_m C_2 R_L + sL_m}{s^2 L_{r2} C_2 + s^2 L_m C_2 + sR_L C_2 + 1} \right)}. \quad (14)$$

Let $s = j\omega$, then the output voltage gain and its partial differential equations to ω are expressed:

$$Gain = f(\omega, L_m), \quad (15)$$

$$\frac{\partial f(\omega, L_m)}{\partial \omega} = 0. \quad (16)$$

To simplify the analysis, here, we assume that the source coil and device coil are identical. Thus, $L_r = L_{r1} = L_{r2}$ and $C_r = C_1 = C_2$. Substitute (14) into (16), and solve the differential

equations. The critical frequency is gotten as following:

$$f_{r0} = \frac{1}{2\pi\sqrt{L_r C_r}}, \quad (17)$$

$$f_{r1} = \frac{1}{2\pi\sqrt{(L_r + 2L_m)C_r}}, \quad (18)$$

$$f_{r2} = \frac{1}{2\pi\sqrt{(L_r + L_m)C_r}}. \quad (19)$$

where $L_m = k^2 L_1$, $L_r = L_1 - L_m$, and k is the coupling coefficient of coils. Thus, the native resonant frequency f_{r0} , the odd splitting frequency f_{r1} , and the even splitting frequency f_{r2} are derived from the T-type transformer model. Figure 3 is the simulation plot of frequency splitting using the parameter values in Table I.

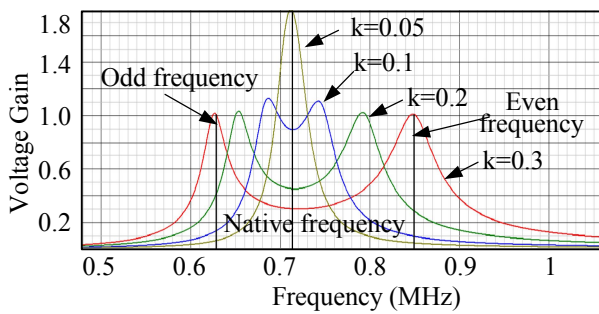


Fig. 3. Frequency splitting phenomena.

TABLE I. THE SIMULATION PARAMETERS.

Parameter	Value	Unit
C_{r1}	2	nF
L_1	25	μ H
R_L	5	Ω
L_2	25	μ H
C_{r2}	2	nF

In Fig. 3, when the coupling k is 0.05, there is a single voltage-peak, while the voltage gain curve appears double voltage-peak when the coupling coefficient increases. Thus, the WPT system enters into the frequency splitting region. Furthermore, it can also be seen that when the system operates in frequency splitting region, the voltage peaks are at the odd frequency and even frequency; and at its native resonant frequency, the voltage gain curve reaches the bottom.

III. ANALYSIS

The schematic diagram of the experimental WPT system is shown in Fig. 4. The half-bridge inverter is implemented to drive the source coil of the WPT system.

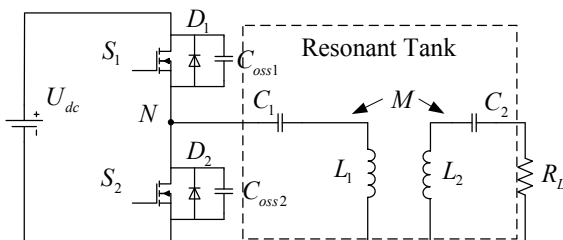


Fig. 4. WPT system based on half-bridge inverter.

In Fig. 4, the MOSFET switches S_1 and S_2 are driven

alternatively with 50 % duty cycle, and the square wave voltage is produced at the mid-node (point N in the Fig. 4.) of the half-bridge inverter. The capacitor C_1 , C_2 and the two coils form a resonant tank are shown within the dash line. In the resonant tank, only sinusoidal current is allowed to flow through because the network filters harmonic currents. The currents in source coil and device coil are with the same frequency. So the two coils resonate with each other. Thus, the energy transfers from source coil to device coil. In addition, this experimental setup uses two identical coils shown in Fig. 5. The litz wire is used to manufacture the coils because of its low series resistor under high frequency operation. The key parameter values are listed in Table II.

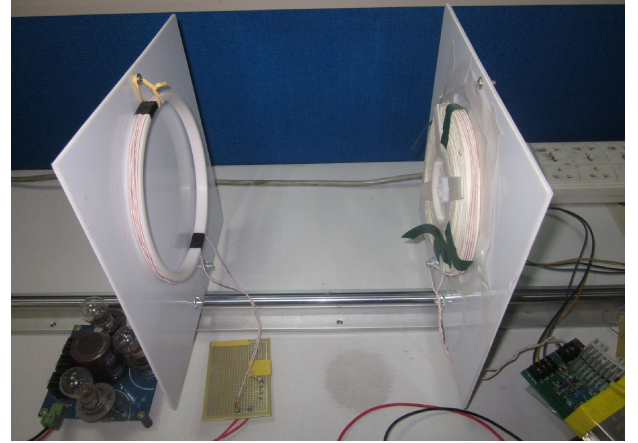


Fig. 5. Experimental setup of WPT system.

TABLE II. THE EXPERIMENTAL SETUP PARAMETERS.

Parameter	Value	Unit
C_1	470	pF
L_1	48	μ H
R_L	10	Ω
L_2	47	μ H
C_2	470	pF

A. Zero Voltage Switching

To acquire the maximum transfer power, the WPT system should operate in high frequency, normally more than 1 MHz. But, when improving operational frequency, the efficiency will drop. Therefore the zero voltage switching (ZVS) in a WPT system must be ensured. The system working under inductive region can realize the ZVS of MOSFETs in voltage-source half-bridge inverter. However, the assumption of working under inductive region is just a necessary condition for ZVS but not sufficient. This is because the parasitic capacitance of the MOSFETs needs energy to be charged and discharged during one switching period. To allow ZVS, a dead time T_{dead} is inserted between the end of the ON-time of a switch and beginning of the ON-time of another one. To ensure discharging the energy of parasitic capacitance completely, the dead time T_{dead} should be larger than the discharging time T_{dis}

$$T_{dead} > T_{dis}. \quad (20)$$

The discharging time T_{dis} can be expressed by (21)

$$t_c = (2C_{oss} + C_{stray}) \frac{V_{dc}}{i_1(T/2)}. \quad (21)$$

In which

$$\begin{cases} i(T/2) = \frac{\sqrt{2}U_{out}^2 \tan \varphi}{RU_{rms}}, \\ \varphi = \arctan \left(\frac{\text{Im } Z_r - \frac{1}{\omega C_p} + \omega L_p}{\text{Re } Z_r} \right). \end{cases} \quad (22)$$

The parasitic capacitance C_{oss} and C_{stray} is shown in Fig. 6.

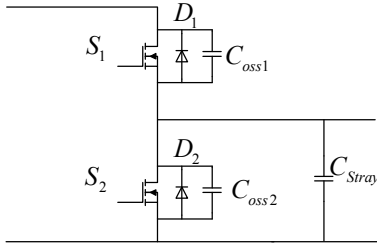


Fig. 6. Zero voltage switching.

The inverter voltage and current in steady-state is shown in Fig. 7(a). In Fig. 7(a), the current lags the inverter voltage which allows the current to pass through the body diodes of

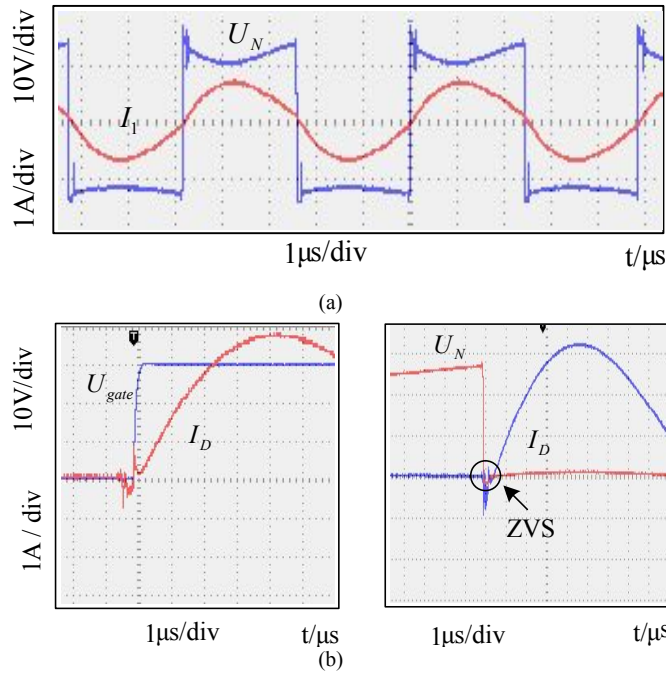


Fig. 7. Zero voltage switching: (a) Inverter current and voltage in steady-state; (b) ZVS switching.

The experimental data of load peak-voltage is shown as the black dot while the theoretical values, calculated from (14) are drawn as blue continuous lines. When coupling increases, frequency splitting phenomena appear. The critical splitting coupling is around $k=0.015$. The load voltage shows a single-peak curve in the region $k < 0.015$; when k increases and is greater than $k < 0.015$, the load voltage curve splits into two curves, and the greater the coupling k , the greater the gap between the odd frequency and the even frequency. As shown in Fig. 6, the experimental results consist with the theoretical values with slight differences.

MOSFETs. When current passes through diodes, the voltage of MOSFETs is clamped to zero. If parasitic capacitance has been discharged completely during the dead time zone, the ZVS can achieve what is shown in Fig. 7(b).

B. Frequency Splitting

The load voltage is measured to demonstrate the frequency splitting phenomena. We slowly move the device coil to be close to the source coil step by step, and in each step the operation frequency sweeps from 500 kHz to 2 MHz. Then, the voltage gain of load is recorded at each step. The experimental results and theoretical values are drawn in the same plot shown in Fig. 6.

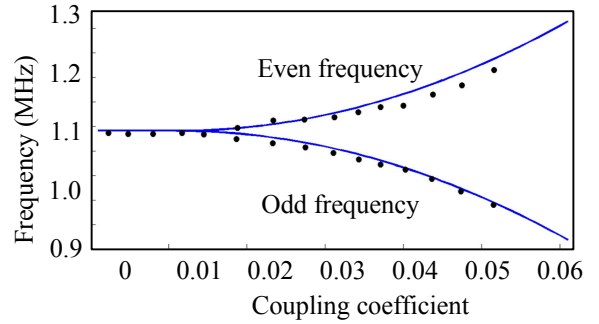


Fig. 8. Experimental results.

IV. DISCUSSION

The frequency bifurcation is discussed frequently in inductively coupled power transfer (ICPT) system which has some same characteristics, but they are different. Frequency bifurcation phenomena are the input characteristics of an ICPT system, while frequency splitting phenomena concerns the output characteristics of WPT systems, although they often appear at the same time. To let the imaginary part of the input impedance to be zero is to define the frequency bifurcation. Bifurcation phenomena are related to the study of

the system stability of a WPT system. There are some stability regions and instability regions in a WPT system with bifurcation. Every operating region has different transfer characteristics.

V. CONCLUSIONS

Frequency splitting phenomena in WPT systems are studied by an electric circuit model method. A simple T-type transformer model is introduced. With impedance analysis, the even and odd splitting frequencies have been derived. In addition, the simulation by the aid of computer shows the output characteristic of frequency splitting. Furthermore, the half-bridge inverter is constructed to drive the WPT system. The ZVS conditions are discussed as well. Finally, the theoretical results are validated by the experimental results. The control method is proposed as well.

REFERENCES

- [1] K. Wu, D. Choudhury, H. Matsumoto, "Wireless power transmission, technology, and applications [Scanning the issue]", in *Proc. IEEE*, vol. 101, 2013, pp. 1271–1275. [Online]. Available: <http://dx.doi.org/10.1109/JPROC.2013.2257590>
- [2] S. Paulikas, P. Sargautis, V. Banevicius, "Impact of wireless channel parameters on quality of video streaming", *Elektronika ir Elektrotechnika (Electronics and Electrical Engineering)*, no. 2, pp. 27–30, 2011.
- [3] R. Radvan, B. Dobrucký, M. Frivaldský, P. Rafajdus, "Modelling and design of HF 200kHz transformers for hard- and soft switching application", *Elektronika ir Elektrotechnika (Electronics and Electrical Engineering)*, no. 4, pp. 7–12, 2011.
- [4] S. Hui, W. Zhong, C. Lee, "A critical review of recent progress in mid-range wireless power transfer", *IEEE Trans. On Power Electronics*, vol. PP, pp. 1–1, 2013.
- [5] A. Kurs, A. Karalis, R. Moffatt, J. D. Joannopoulos, P. Fisher, M. Soljacic, "Wireless power transfer via strongly coupled magnetic resonances", *Science*, vol. 317, pp. 83–6, Jul 6 2007. [Online]. Available: <http://dx.doi.org/10.1126/science.1143254>
- [6] J. Gozalvez, "WiTricity-the wireless power transfer [Mobile radio]", *Vehicular Technology Magazine IEEE*, vol. 2, pp. 38–44, 2007. [Online]. Available: <http://dx.doi.org/10.1109/MVT.2007.913285>
- [7] A. P. Sample, D. A. Meyer, J. R. Smith, "Analysis, experimental results, and range adaptation of magnetically coupled resonators for wireless power transfer", *IEEE Trans. on Industrial Electronics*, vol. 58, pp. 544–554, 2011. [Online]. Available: <http://dx.doi.org/10.1109/TIE.2010.2046002>
- [8] B. L. Cannon, J. F. Hoburg, D. D. Stancil, S. C. Goldstein, "Magnetic resonant coupling as a potential means for wireless power transfer to multiple small receivers", *IEEE Trans. on Power Electronics*, vol. 24, pp. 1819–1825, 2009. [Online]. Available: <http://dx.doi.org/10.1109/TPEL.2009.2017195>
- [9] T. Youndo, P. Jongmin, N. Sangwook, "Mode-based analysis of resonant characteristics for near-field coupled small antennas", *Antennas and Wireless Propagation Letters, IEEE*, vol. 8, pp. 1238–1241, 2009. [Online]. Available: <http://dx.doi.org/10.1109/LAWP.2009.2036133>
- [10] T. Imura, Y. Hori, "Maximizing air gap and efficiency of magnetic resonant coupling for wireless power transfer using equivalent circuit and neumann formula", *IEEE Trans. on Industrial Electronics*, vol. 58, pp. 4746–4752, 2011. [Online]. Available: <http://dx.doi.org/10.1109/TIE.2011.2112317>
- [11] Y. Kim, H. Ling, "Investigation of coupled mode behaviour of electrically small meander antennas", *Electronics Letters*, vol. 43, 2007.
- [12] C. Linhui, L. Shuo, Z. Yong Chun, C. Tie Jun, "An optimizable circuit structure for high-efficiency wireless power transfer", *IEEE Trans. on Industrial Electronics*, vol. 60, pp. 339–349, 2013. [Online]. Available: <http://dx.doi.org/10.1109/TIE.2011.2179275>
- [13] C. Sanghoon, K. Yong-Hae, S.-Y. Kang, L. Myung-Lae, L. Jong-Moo, T. Zyung, "Circuit-model-based analysis of a wireless energy-transfer system via coupled magnetic resonances", *IEEE Trans. on Industrial Electronics*, vol. 58, pp. 2906–2914, 2011. [Online]. Available: <http://dx.doi.org/10.1109/TIE.2010.2072893>
- [14] M. Kiani, M. Ghovanloo, "The circuit theory behind coupled-mode magnetic resonance-based wireless power transmission", *IEEE Trans. on Circuits and Systems I: Regular Papers*, vol. 59, pp. 2065–2074, 2012.
- [15] B. Ose-Zal, E. Jakobsons, P. Suskis, "The use of magnetic coupler instead of lever actuated friction clutch for wind plant", *Elektronika ir Elektrotechnika (Electronics and Electrical Engineering)*, no. 10, pp. 13–16, 2012.
- [16] M. W. Baker, R. Sarpeshkar, "Feedback analysis and design of rf power links for low-power bionic systems", *IEEE Trans. on Biomedical Circuits and Systems*, vol. 1, pp. 28–38, 2007. [Online]. Available: <http://dx.doi.org/10.1109/TBCAS.2007.893180>
- [17] N. Wang-Qiang, C. Jian-Xin, G. Wei, S. Ai-Di, "Exact analysis of frequency splitting phenomena of contactless power transfer systems", *IEEE Trans. on Circuits and Systems I: Regular Papers*, vol. 60, pp. 1670–1677, 2013.
- [18] W. Q. Niu, W. Gu, J. X. Chu, A. D. Shen, "Coupled-mode analysis of frequency splitting phenomena in CPT systems", *Electronics Letters*, vol. 48, pp. 723–724, 2012. [Online]. Available: <http://dx.doi.org/10.1049/el.2012.0953>